Research Square

Preprints are preliminary reports that have not undergone peer review.
They should not be considered conclusive, used to inform clinical practice,
or referenced by the media as validated information.

Hyperglycemia Aggravates Blood–Brain Barrier Disruption Following Diffuse Axonal Injury by Increasing the Levels of Inflammatory Mediators through the PPARγ/Caveolin-1/TLR4 Pathway

Xing Wei
the Second Affiliated Hospital of Xi'an Jiaotong University
Yaqing Zhou
the Second Affiliated Hospital of Xi'an Jiaotong University
Jinning Song
the First Affiliated Hospital of Xi'an Jiaotong University
Junjie Zhao
the Second Affiliated Hospital of Xi'an Jiaotong University
Tingqin Huang
the Second Affiliated Hospital of Xi'an Jiaotong University
Ming Zhang
the Second Affiliated Hospital of Xi'an Jiaotong University
Yonglin Zhao (zhaoyonglinlin@163.com)
the Second Affiliated Hospital of Xi'an Jiaotong University

Research Article

Keywords: Hyperglycemia, Peroxisome proliferator-activated receptor γ, Blood–brain barrier, Diffuse axonal injury

Posted Date: May 10th, 2022

DOI: https://doi.org/10.21203/rs.3.rs-1618675/v1

License: This work is licensed under a Creative Commons Attribution 4.0 International License.
Read Full License

Abstract

Hyperglycemia aggravates brain damage after diffuse axonal injury (DAI), but the underlying mechanisms are not fully defined. In this study, we aimed to investigate a possible role for hyperglycemia in the disruption of blood–brain barrier (BBB) integrity in a rat model of DAI and the underlying mechanisms. Accordingly, 50% glucose was intraperitoneally injected after DAI to establish the hyperglycemia model. Hyperglycemia treatment aggravated neurological impairment and axonal injury, increased cell apoptosis and glial activation, and promoted the release of inflammatory factors, including TNF-α, IL-1β, and IL-6. It also exacerbated BBB disruption and decreased the expression of tight junction-associated proteins, including ZO-1, claudin-5, and occludin-1, whereas the PPARγ agonist rosiglitazone (RSG) had the opposite effects. An in vitro BBB model was established by a monolayer of human microvascular endothelial cells (HBMECs). Hyperglycemia induction worsened the loss of BBB integrity induced by oxygen and glucose deprivation (OGD) by increasing the release of inflammatory factors and decreasing the expression of tight junction-associated proteins. Hyperglycemia further reduced the expression of PPARγ and caveolin-1, which significantly decreased after DAI and OGD. Hyperglycemia also further increased the expression of toll-like receptor 4 (TLR4), which significantly increased after OGD. Subsequently, the PPARγ agonist RSG increased caveolin-1 expression and decreased TLR4 expression and inflammatory factor levels. In contrast, caveolin-1 siRNA abrogated the protective effects of RSG in the in vitro BBB model of hyperglycemia by increasing TLR4 and Myd88 expression and the levels of inflammatory factors, including TNF-α, IL-1β, and IL-6. Collectively, we demonstrated that hyperglycemia was involved in mediating secondary injury after DAI by disrupting BBB integrity by inducing inflammation through the PPARγ/caveolin-1/TLR4 pathway.

1. Introduction

Diffuse axonal injury (DAI), an important pathoanatomical subgroup of traumatic brain injury (TBI), refers to intracranial injury caused by rapid and sustained deceleration or acceleration of the brain, leading to higher mortality and functional impairment. DAI is believed to be involved in sustaining loss of consciousness due to a motor vehicle crash after TBI[1]. Pathologically, despite primary mechanical breaking of the axonal cytoskeleton, DAI encompasses a spectrum of abnormalities ranging from inflammation, intracellular calcium overload, transport interruption, swelling, and proteolysis through secondary physiological changes[2].

TBI, especially DAI, can induce many complications, including epilepsy, hydrocephalus, sleep disorders, pulmonary infections, deep vein thrombosis, cerebral hernia, and hyperglycemia. Hyperglycemia related to diabetes is less important than stress-induced hyperglycemia in terms of mortality in acute trauma and TBI patients[3]. TBI patients with hyperglycemia have a poor prognosis and an increased risk of mortality. Findings from a previous study suggest that a glucose level > or = 160 mg/dl within the first 24 h of admission following TBI is associated with poor outcomes irrespective of the severity of injury[4].

The causes of hyperglycemia after TBI might be related to the stress response, the inflammatory response, diabetes mellitus, surgery and so on[5]. The main reason that persistent hyperglycemia leads to a poor prognosis may be because of a series of pathological changes, and rupture of the BBB is an important pathogenic mechanisms[5]. At present, many cures and remedies are available for hyperglycemia after TBI. However, these measures do not seem to improve the prognosis of TBI[6]. For example, intensive glycemic control could improve neurological outcomes, decrease the infection rate and reduce the LOS in the ICU[5]. However, intensive glycemic therapy will not affect mortality in TBI patients[7]. Although research on the relationship between hyperglycemia and severe TBI has achieved considerable progress in recent years, the complete mechanism requires further study.

Peroxisome proliferator activated receptor gamma (PPARγ) belongs to the family of ligand-regulated nuclear receptors. Rosiglitazone (RSG), a PPARγ agonist, has been shown to exert a neuroprotective effect in TBI, focal cerebral ischemia, and subarachnoid hemorrhage[8]. Our previous study showed that the PPARγ agonist RSG can protect BBB integrity by decreasing the levels of inflammatory mediators through a caveolin-1-dependent pathway. However, whether RSG plays a protective role against DAI with hyperglycemia and the underlying mechanisms remain elusive[9].

In the present study, the effects of hyperglycemia on neurological impairment, axonal injury, cell apoptosis, glial response, BBB integrity, and the level of inflammatory factors in DAI were explored. We also assessed the expression and role of PPARγ in the expression of caveolin-1 and tight junction-associated proteins after DAI in vivo and OGD in vitro after hyperglycemia treatment. Finally, to study the downstream signal transduction mechanisms of caveolin-1, the expression of TLR4/Myd88 pathway-related proteins was detected by downregulating caveolin-1. All results showed that hyperglycemia was involved in mediating secondary injury after DAI by disrupting BBB integrity by inducing inflammation through the PPARγ/caveolin-1/TLR4 pathway.

2. Experimental Procedures

2.1 Animals and Experimental Groups

Male Sprague–Dawley (SD) rats were supplied by the Experimental Animal Center of Xi'an Jiaotong University [license no. SCXK (Shaanxi) 2006-001]. Rats (weighing 250–300 g, 8–10 weeks old) were raised at 24 ± 1°C under a 12-h/12-h light/dark cycle with free access to food and water. All procedures were performed according to the Guidelines and Suggestions for the Care and Use of Laboratory Animals formulated by the Ministry of Science and Technology of the People's Republic of China. All protocols were approved by the Biomedical Ethics Committee of Medical College of Xi'an Jiaotong University of China (2014 – 124).

A total of 132 SD rats were divided into the following groups: the control group (30 rats), DAI 1 d group (30 rats), DAI 1 d + hyperglycemia (HG) group (30 rats), and DAI 1 d + HG + rosiglitazone (RSG) group (30 rats), DAI 6 h group (6 rats) and DAI 3 d group (6 rats). RSG (2 mg/mL, Cayman Chemical Co., Ann Arbor,

MI, USA) was intraperitoneally injected after DAI and glucose treatment at a dose of 10 mg/kg, followed by repeated injections every 12 h[10]. Rats subjected to hyperglycemia were intraperitoneally injected with glucose (6.0 mL/kg; 50% glucose) at 0 h and 12 h postinjury[11]. Blood samples were obtained by tail venipuncture at various times pre- and postinjection for 24 h (0, 6 h, 12 h, 18 h, and 24 h) and used to determine blood glucose concentrations. Glucose levels were maintained at > 16.8 mmol/L within 24 h after injury[12].

2.2 Animal DAI Model

The DAI model was established by a lateral head-rotation device as described in previous studies[10, 13, 14]. Briefly, after anesthesia with 1% pentobarbital sodium (35 mg/kg), the rat head was horizontally fixed to the lateral head-rotation device by two lateral ear bars, with the body positioned. When the trigger was pushed, the rat head was rapidly rotated 90°, leading to sudden acceleration and deceleration. All injured rats were in a coma for at least 30 minutes. The control rats underwent only anesthesia and fixation to the device and were not subjected to injury.

2.3 Hematoxylin and Eosin (H&E) Staining

After anesthesia and perfusion with normal saline and 40 g/L paraformaldehyde, brains were paraffin embedded and subjected to routine H&E staining, and the morphology was observed by a light microscope.

2.4 Immunohistochemical Staining and Semiquantitative Analysis

Brain sections were deparaffinized and rehydrated. Endogenous peroxidase activity was quenched for 15 minutes, followed by a wash in PBS. Sections were incubated with β-amyloid precursor protein (β-APP) antibody, glial fibrillary acidic protein (GFAP) antibody, ionized calcium-binding adapter molecule-1 (Iba-1) antibody, neurofilament light chain (NF-L) antibody, and neurofilament heavy chain (NF-H) antibody at 4°C overnight. Then, the sections were covered with secondary antibody for 20 minutes at 37°C. The signal was developed with streptoavidine and revealed with 3,30-diaminobenzidine. The results were observed under a microscope at 40x magnification. The result of immunohistochemical staining was assessed by immunohistochemical scores, which were determined by the quantity and staining intensity scores. The quantity scores were rated from 0 to 4: no staining, 0; 1–10% of cells stained, 1; 11–50%, 2; 51–80%, 3; and 81–100%, 4; the staining intensity scores were rated from 0 to 3: with 0, negative; 1, weak; 2, moderate; and 3, strong. Theoretically, the total scores obtained by multiplying the quantity and staining intensity scores could range from 0 to 12 [10, 15].

2.5 Terminal Deoxynucleotidyl Transferase dUTP Nick-End Labeling (TUNEL) Assay

The TUNEL method was used to measure apoptotic cells with the DeadEnd Fluorometric TUNEL System (Promega, Madison, WI, USA) according to the instructions. Six fields were randomly selected from the rat

cortex to count the TUNEL-positive cells.

2.6 Western Blotting

The concentration of total protein isolated from the myocardium was measured by the bicinchoninic acid method. Equivalent amounts of proteins from each sample were separated by 10% SDS/PAGE gels and then transferred to polyvinylidene fluoride (PVDF) membranes. Membranes were blocked for nonspecific binding and probed with primary antibodies, including caveolin-1 antibody (1:1000), ZO-1 antibody (1:1000), claudin-5 antibody (1:1000), β-actin antibody (1:1000), occludin-1 antibody (1:1000), PPARγ antibody (1:1000), MyD88 antibody (1:500) and TLR4 antibody (1:500), at 4°C overnight. Then, the membranes were incubated with HRP-conjugated anti-mouse IgG antibody or anti-rabbit antibody for 1 h at room temperature. An ECL chemiluminescence kit was used to visualize the specific blots, and autoradiograms were quantified by densitometry.

2.7 Immunofluorescence Staining

Sections were deparaffinized and rehydrated before inactivating endogenous peroxidase and then blocked with serum after antigen unmasking. Rat brain sections were then incubated overnight at 4°C with primary antibodies, including caveolin-1 antibody (1:400) and ZO-1 antibody (1:200). The sections were washed and incubated with fluorochrome-conjugated secondary antibody and DAPI and then observed under a fluorescence microscope.

2.8 BBB Permeability Assay

The penetration of Evans blue was used to assess BBB permeability. Evans blue (2%, Sigma–Aldrich, St. Louis, MO, USA) was intravenously administered (4 mL/kg of body weight) via the tail vein 1 h before measurement. After circulation, the rat was transcardially perfused with saline, and the brain was quickly removed. The EB content was determined as previously described[10].

2.9 Evaluation of Brain Edema

To evaluate the brain water content (BWC), the wet-dry method was employed. Briefly, the brain wet weight was recorded. The brains were then dried in an oven at 105°C for 72 h, and their dry weight was determined. Brain water content (%) was derived as (wet weight − dry weight)/wet weight×100%.

2.10 Cell Culture, Oxygen-Glucose Deprivation (OGD) and Treatment

Human brain microvascular endothelial cells (HBMECs) were grown as a monolayer in culture medium containing 10% fetal bovine serum at 37°C in a humidified atmosphere with 5% CO_2 and 95% air. Cells were divided into the following groups: control group, OGD 3 h group, OGD 6 h group, OGD 9 h group, OGD 6 h + HG group, OGD 6 h + HG + RSG group, and OGD 6 h + HG + RSG + cav-1 siRNA group. To establish an OGD model in vitro, the cells were exposed to a gas mixture of 95% N_2/5% CO_2 at 37°C for 1 h, and growth media was replaced with 10% FBS DME media without glucose. RSG was added 30 min

before OGD[10, 16]. In the hyperglycemia (HG) groups, primary HBMECs were cultured on the inner surface of collagen-coated Transwell inserts in complete culture containing 25 mM glucose[17]. After OGD, conditioned media were collected, and the cells were harvested for further experiments.

2.11 Small interfering RNA (siRNA) transfection

SiRNA transfection was performed in vitro according to the protocol described in previous studies[10, 18]. HBMECs were transfected with 100 pmol of siRNA (sc-29241, Santa Cruz Biotech, Santa Cruz, CA, USA) at 70–80% confluence according to the manufacturer's instructions. After 6 h, the culture was replaced with fresh medium, and the cells were grown for another 24 h. Twenty-four hours after transfection, the cells were subjected to OGD and other treatments.

2.12 Transendothelial Electrical Resistance (TEER) Measurement

TEER was performed according to the protocol described in previous studies[10]. A Millicell-ERS instrument (Millipore, Billerica, MA, USA) was used to measure TEER. The resistance of blank filters was subtracted from that of cell-coated filters before the final resistance values were calculated [19]. The TEER values were measured in $\mu\Omega/cm^2$.

2.13 Peroxisome Proliferator-activated Receptor 843 Horseradish Peroxidase (HRP) Flux

HRP flux experiments were used to measure BBB permeability in vitro. Serum-free culture media containing 0.5 μM HRP (Sigma–Aldrich, St. Louis, MO, USA) were added to the upper compartment of the transwells. The amount of HRP was quantified as described previously[10, 20]. HRP flux was assumed to be in nanograms per milliliter.

2.14 Enzyme-linked Immunosorbent Assay (ELISA).

The levels of tumor necrosis factor-α (TNF-α), interleukin- (IL-) 1β, and IL-6 were detected by ELISA kits (R&D Systems, Minneapolis, MN, USA) according to the manufacturer's instructions. Data (pg protein) were normalized to milligrams of total protein.

2.15 Neurobehavioral evaluation

Neurological deficit scores were evaluated in the control group, DAI 1 d group, DAI 1 d + HG group, and DAI 1 d + HG + RSG group by employing the modified neurological severity scoring (mNSS) system by a blinded investigator. The mNSS is a composite of motor, sensory, and reflex tests and has been employed in previous studies[21, 22]. Neurological function is graded on a scale of 0 to 18, with a higher score corresponding to more severe injury.

2.16 Statistical Analysis

Data are presented as the mean ± SD, and statistical analyses were performed with SPSS 18.0 (SPSS, Chicago, IL, USA). Numerical data were analyzed by one-way ANOVA to compare more than 2 groups, followed by the LSD (L) test for post hoc analysis. A P value < 0.05 denoted a significant difference.

3. Results

3.1 Glucose levels and neurological outcomes in hyperglycemic rats were ameliorated by RSG treatment after DAI

Blood glucose levels were significantly higher in rats in the DAI 1 d group, DAI 1 d + HG group, and DAI 1 d + HG + RSG group compared with those in the control group. The blood glucose level of rats detected in the DAI 1 d + HG group was significantly increased compared with that in the DAI 1 d group. Compared with the DAI 1 d + HG group, RSG treatment decreased the blood glucose levels after DAI suffering hyperglycemia (Fig. 1A).

Compared with that in the control group, the mNSS score was higher in the DAI 1 d group, indicating that DAI significantly induced neurological impairment on Day 1. A significant elevation in the mNSS score was found in the hyperglycemia-treated rats compared to the DAI 1 d group rats, suggesting that significant sensorimotor functional impairment occurred after hyperglycemia induction. However, compared with that in the DAI 1 d + HG group, functional recovery was significantly increased in the DAI 1 d + HG + RSG group (Fig. 1B).

3.2 Activation of PPARγ alleviated hyperglycemia-induced axonal injury after DAI

In H&E-stained sections, cells were intact, and cell structures were clear in the control group. Nuclear fragmentation and pyknotic, swollen, and tangled neurons were observed in the DAI 1 d group. Hyperglycemia aggravated the pathological damage described above at 1 d after DAI, while in the DAI 1 d + HG + RSG group, abnormal histopathological changes were relieved. β-APP, NF-L, and NF-H are considered markers of axonal damage. Compared to those in the control group, β-APP, NF-L and NF-H expression levels were significantly increased in the cortices of the DAI 1 d group rats. Hyperglycemia increased the expression of β-APP, NF-L, and NF-H in the DAI 1 d + HG group. Compared with that in the DAI 1 d + HG group, the expression of β-APP, NF-L, and NF-H was decreased in the DAI 1 d + HG + RSG group (Fig. 2). The results suggest that hyperglycemia exacerbated axonal injury after DAI, and PPARγ activation alleviated hyperglycemia-induced axonal injury.

3.3 Effects of hyperglycemia and PPARγ activation on glial responses and cell apoptosis

A TUNEL assay was used to assess cell apoptosis. The expression of the microglial cell biomarker Iba-1 and the astrocyte biomarker GFAP was detected by immunohistochemical staining. Few TUNEL-positive cells, Iba-1-positive cells and GFAP-positive cells were detected in the control group. Compared to those in the control group, the number of TUNEL-positive cells and the expression of Iba-1 and GFAP were increased in the cortex in the DAI 1 d group. Compared to those in the DAI 1 d group, the number of TUNEL-positive cells and the expression of Iba-1 and GFAP were significantly increased in the DAI 1 d + HG group, whereas RSG treatment decreased the number of TUNEL-positive cells and the expression of Iba-1 and GFAP after DAI and hyperglycemia induction (Figs. 3, 4).

3.4 Dynamic expression of PPARγ after DAI and OGD under hyperglycemic conditions

Western blotting was performed to examine PPARγ expression at different time points after DAI and OGD. Compared with that in the control group, PPARγ expression was significantly decreased in the DAI 6 h group, reaching a minimum in the DAI 1 d group and then gradually increasing in the DAI 3 d group (Fig. 5A). Similarly, compared with that in the control group, PPARγ expression was significantly decreased in the OGD 3 h group, reaching a minimum in the OGD 6 h group and then stabilizing in the OGD 9 h group (Fig. 5C). After hyperglycemia treatment, compared to that in the DAI 1 d group, PPARγ expression was further decreased in the DAI 1 d + HG group, and compared to that in the OGD 6 h group, PPARγ expression was further decreased in the OGD 6 h + HG group (Fig. 5B, 5D).

3.5 The roles of hyperglycemia and PPARγ in the regulation of BBB permeability and integrity in vivo and in vitro

The immunofluorescence staining results showed that ZO-1 expression was decreased following DAI, and hyperglycemia worsened the decrease in ZO-1, indicating that the BBB was further disrupted, which was accompanied by hyperglycemia, after DAI. RSG treatment resulted in significantly higher levels of ZO-1 expression than DAI 1 d + HG treatment (Fig. 6A). Evans blue and BWC were used to monitor BBB destruction and brain edema. Compared with observations in the control group, DAI induced significant brain edema and leakage of Evans blue, which was significantly aggravated by hyperglycemia treatment in the DAI 1 d + HG group, whereas RSG relieved cerebral edema and decreased Evans blue diffusion in the DAI 1 d + HG + RSG group (Fig. 6B).

In vitro, after OGD for 6 h, the expression of occludin-1, ZO-1, and claudin-5 was decreased compared to that in the control group. Meanwhile, hyperglycemia significantly decreased the expression of TJ proteins compared with that in the OGD 6 h group, while RSG treatment reversed the decrease in the expression of TJ proteins induced by hyperglycemia (Fig. 7A). Compared with those in the control group, the TEER decreased, whereas the HRP flux increased in the OGD 6 h group. Hyperglycemia significantly decreased TEER and increased HRP flux compared with observations in the OGD 6 h group. Compared with those in the OGD 6 h + HG group, RSG treatment significantly increased TEER and decreased HRP flux in the OGD 6 h + HG + RSG group (Fig. 7B, 7C).

3.6 RSG decreased the level of inflammatory cytokines through the caveolin-1/TLR4 pathway after DAI and hyperglycemia induction

In vivo, compared with that in the control group, caveolin-1 expression in the DAI 1 d group was slightly higher after DAI, and hyperglycemia significantly reduced caveolin-1 expression in the DAI 1 d + HG group, while this change could be reversed by RSG treatment in the DAI 1 d + HG + RSG group (Fig. 8A). Compared with those in the control group, the levels of TNF-α, IL-1β, and IL-6 were increased in the DAI 1 d group. When compared with those in the DAI 1 d group, the levels of TNF-α, IL-1β, and IL-6 were increased in the DAI 1 d + HG group, while RSG decreased the levels of inflammatory mediators in the DAI 1 d + HG + RSG group (Fig. 8B).

In vitro, compared with those in the control group, caveolin-1 expression was reduced, and TLR4 expression and the levels of inflammatory mediators, including TNF-α, IL-1β, and IL-6, were increased in the OGD 6 h group. In contrast to those in the OGD 6 h group, hyperglycemia significantly reduced caveolin-1 expression and increased TLR4 expression and the levels of TNF-α, IL-1β, and IL-6 in the OGD 6 h + HG group. After RSG treatment, caveolin-1 expression was increased, and TLR4 expression and the levels of TNF-α, IL-1β, and IL-6 were decreased in the OGD 6 h + HG + RSG group (Fig. 9A, 9C). Cav-1 siRNA was used to downregulate caveolin-1 expression. Compared with those in the OGD 6 h + HG + RSG group, TLR4 and Myd88 expression and the levels of TNF-α, IL-1β, and IL-6 were all increased in the OGD 6 h + HG + cav-1 siRNA + RSG group (Fig. 9B, 9D). These results indicate that hyperglycemia disrupted the BBB model by increasing the expression levels of inflammatory cytokines through the PPARγ/caveolin-1/TLR4 pathway after DAI.

Discussion

Hyperglycemia (both peak glucose and persistent hyperglycemia) in TBI patients is associated with injury severity and clinical outcomes[7, 23, 24]. Previous studies have shown that primary trauma evokes a cascade of changes that result in secondary axonal injury[25]. The role of blood glucose in the secondary mechanisms of neuronal damage after DAI has not yet been clarified. In this study, we found that abnormal histopathological changes were exacerbated when DAI rats suffered hyperglycemia. Meanwhile, the expression of markers of axonal damage, including β-APP, NF-L, and NF-H, and the number of TUNEL-positive cells were increased significantly in DAI rats with hyperglycemia, indicating that hyperglycemia led to more serious secondary axonal damage after DAI. Similarly, the link between hyperglycemia and a poor prognosis is also observed in ischemic stroke, subarachnoid hemorrhage, intracerebral hemorrhage and other neurodegenerative diseases.

Next, the mechanisms underlying hyperglycemia leading to secondary damage after DAI were studied. Persistent hyperglycemia results in acidosis, electrolyte disturbances, inflammation, vessel disorders, BBB rupture, and hyperpermeability. The BBB is a highly specialized arrangement of the vasculature that has evolved to provide protection from potentially harmful pathogens that enter the bloodstream[26, 27]. In many CNS diseases, such as stroke and subarachnoid hemorrhage, loss of BBB tight junction integrity leads to increased paracellular permeability[26, 27]. Vascular endothelial cells are a significant target of

hyperglycemic damage, but the mechanisms underlying such damage to the cerebral microvasculature are not fully understood[28, 29]. In this study, a possible role of hyperglycemia in the regulation of BBB integrity following DAI was investigated. Hyperglycemia aggravated DAI-induced significant brain edema and Evans blue leakage in vivo, and OGD induced a decrease in TEER and increased HRP flux in vitro. The damage to BBB permeability caused by hyperglycemia contributed to a decrease in tight junction proteins, including occludin-1, ZO-1, and claudin-5. Meanwhile, previous studies have also reported that hyperglycemia leads to endothelial dysfunction and cerebrovascular changes during both ischemia and reperfusion[30, 31]. However, the role of hyperglycemia in the secondary mechanisms of BBB damage after DAI has not yet been clarified.

Neuroinflammation is an important common determinant of increased BBB permeability. PPARγ is a subunit of PPAR and is a ligand-activated nuclear transcription factor. PPARγ can be activated by its ligand. PPARγ ligands attenuate degenerative processes in the brain through the control of anti-inflammatory mechanisms, oxidative stress, neuronal death, neurogenesis, differentiation, and angiogenesis[32]. Once activated, PPARγ can combine with specific DNA response elements to regulate the transcription and expression of genes, and neuroinflammation is markedly suppressed in many cerebral injuries[32]. Previous studies have demonstrated that PPAR-γ activation can exert neuroprotective effects on many animal models of acute brain insults and can reduce brain edema. For example, AQP4 deletion protects BBB integrity by reducing inflammatory responses due to upregulation of PPAR-γ expression and attenuation of proinflammatory cytokine release after acute severe hypoglycemia[33]. Our findings indicate that PPARγ activation may alleviate axonal injury by reducing BBB disruption. In this study, PPARγ expression was decreased significantly after DAI and OGD. In the hyperglycemia-treated groups, PPARγ expression was further decreased, indicating that the secondary damage to the BBB induced by hypoglycemia was associated with the reduction in PPARγ expression.

Our previous study also showed that the PPARγ agonist RSG can protect BBB integrity by decreasing the levels of inflammatory mediators through a caveolin-1-dependent pathway. Upregulation of caveolin-1 by RSG has been demonstrated to require superoxide formation and activation of Src, EGFR, and the Mek1-Erk1/2 and p38 MAP kinase pathways[34, 35]. Caveolin-1 is a plasmalemmal anchoring protein and modulator of vascular function and glucose homeostasis. A chronic hyperglycemic condition directly decreased caveolin-1 expression in the brain neurons of diabetic rats, and the downregulation of caveolin-1 induced by chronic hyperglycemic conditions is independent of mTOR signaling[36, 37]. In this study, hyperglycemia significantly reduced caveolin-1 expression after DAI and OGD. After RSG treatment, caveolin-1 expression was increased, but all protective effects of RSG were abrogated when caveolin-1 expression was downregulated. These results indicate that RSG protected BBB integrity by upregulating the expression of TJ proteins through the caveolin-1 pathway after DAI combined with hyperglycemia. In contrast, one study found that high glucose could lead to the hyperpermeability of monolayer endothelial cells through the VEGF/KDR pathway and caveolin-1 overexpression[38]. The role of caveolin-1 in hyperglycemia-induced pathological changes requires further study.

Experimental studies have shown that a hyperglycemic condition activates the production of IL-1, IL-6, and TNF-α[39–41]. All these inflammatory factors have been reported to be related to secondary axonal injury. IL-1β and TNF-α overexpression was strongly related to axonal injury, while IL-6 mRNA and protein expression levels were also positive at sites where axonal injury was observed[42]. Moreover, brain injury itself stimulates systemic inflammation, leading to increased permeability of the BBB, which is exacerbated by secondary brain injury. High glucose has been demonstrated to exacerbate neuroinflammation and apoptosis in the intermediate stage post-TBI by inhibiting the MEK5/ERK5 pathway[24]. In this study, the levels of inflammatory mediators, including TNF-α, IL-1β, and IL-6, were increased after DAI and OGD. Furthermore, hyperglycemia significantly increased TLR4 expression and the levels of TNF-α, IL-1β, and IL-6. After RSG treatment, TLR4 expression and TNF-α, IL-1β, and IL-6 levelswere decreased. Inhibition of caveolin-1 by Cav-1 siRNA abrogated the protective effect of RSG. Thus, RSG protected the BBB model by increasing the expression of TJ proteins and decreasing the levels of inflammatory cytokines through the caveolin-1/TLR4 pathway after DAI combined with hyperglycemia. Our previous findings indicated that TLR4 inhibition at 1 d after DAI effectively alleviated pathological changes, including apoptosis, neuronal and axonal injury, and glial responses, with decreased inflammatory factor levels. Moreover, caveolin-1 could negatively regulate TLR4 activation[43, 44]. Reduced caveolin-1 expression in monocytes could aggravate the TLR4-mediated inflammatory cascade[45]. Studies have also found that cav-1 binds to TLR4 and inhibits lipopolysaccharide-induced proinflammatory cytokine (TNF-α and IL-6) production in murine macrophages. Mutation analysis revealed a caveolin-1 binding motif in TLR4, which is essential for this interaction and for the attenuation of proinflammatory signaling[46].

In conclusion, our findings indicate that hyperglycemia exacerbated axonal injury, cell apoptosis, and glial activation and destroyed BBB integrity by downregulating the expression of TJ proteins and accelerating the release of inflammatory mediators, accompanied by inhibition of PPARγ and activation of the caveolin-1/TLR4 signaling pathways after DAI. Our findings provide evidence that hyperglycemia exerts marked deleterious cerebral effects after DAI and suggest that PPARγ agonists hold considerable promise with respect to new DAI accompanied by hyperglycemia treatment.

Declarations

Ethics approval and consent to participate

All procedures were performed according to the Guidelines and Suggestions for the Care and Use of Laboratory Animals formulated by the Ministry of Science and Technology of the People's Republic of China. All protocols were approved by the Biomedical Ethics Committee of Medical College of Xi'an Jiaotong University of China (2020-124).

Consent for publication

Not applicable

Acknowledgments

We would like to thank Dr. Jinning Song for his valuable input in this article and for reviewing the work.

Data Availability

Some or all data, models, or code generated or used during the study are available in a repository or online in accordance with funder data retention policies (provide full citations that include URLs or DOIs.)

Competing Interests

All of the authors involved in the preparation of the paper declare no conflicts of interest in any form.

Funding Information

This work was financially supported by the National Natural Science Foundation of China (Grant No. 82001327 awarded to Yonglin Zhao).

Author contributions

Xing Wei, Yaqing Zhou, Jinning Song, Yonglin Zhao conceived the concept and drafted the preliminary framework of research. Xing Wei, Yaqing Zhou, Junjie Zhao, Tingqin Huang conducted the experiments and transcribed the data. Xing Wei, Yonglin Zhao wrote the initial draft. Ming Zhang, Yonglin Zhao finalized the results. All authors equally contributed in finalizing the paper.

References

1. Humble SS, Wilson LD, Wang L, et al. Prognosis of diffuse axonal injury with traumatic brain injury[J]. J Trauma Acute Care Surg, 2018, 85 (1): 155–159.
2. Johnson VE, Stewart W, Smith DH. Axonal pathology in traumatic brain injury[J]. Exp Neurol, 2013, 246: 35–43.
3. Bosarge PL, Shoultz TH, Griffin RL, et al. Stress-induced hyperglycemia is associated with higher mortality in severe traumatic brain injury[J]. J Trauma Acute Care Surg, 2015, 79 (2): 289–294.
4. Liu-DeRyke X, Collingridge DS, Orme J, et al. Clinical impact of early hyperglycemia during acute phase of traumatic brain injury[J]. Neurocrit Care, 2009, 11 (2): 151–157.
5. Shi J, Dong B, Mao Y, et al. Review: Traumatic brain injury and hyperglycemia, a potentially modifiable risk factor[J]. Oncotarget, 2016, 7 (43): 71052–71061.
6. Hermanides J, Plummer MP, Finnis M, et al. Glycaemic control targets after traumatic brain injury: a systematic review and meta-analysis[J]. Crit Care, 2018, 22 (1): 11.
7. Zhu C, Chen J, Pan J, et al. Therapeutic effect of intensive glycemic control therapy in patients with traumatic brain injury: A systematic review and meta-analysis of randomized controlled trials[J]. Medicine (Baltimore), 2018, 97 (30): e11671.

8. Govindarajulu M, Pinky PD, Bloemer J, et al. Signaling Mechanisms of Selective PPARγ Modulators in Alzheimer's Disease[J]. PPAR Res, 2018, 2018: 2010675.
9. Zhao Y, Wei X, Song J, et al. Peroxisome Proliferator-Activated Receptor gamma Agonist Rosiglitazone Protects Blood-Brain Barrier Integrity Following Diffuse Axonal Injury by Decreasing the Levels of Inflammatory Mediators Through a Caveolin-1-Dependent Pathway[J]. Inflammation, 2019, 42 (3): 841–856.
10. Zhao Y, Wei X, Song J, et al. Peroxisome Proliferator-Activated Receptor γ Agonist Rosiglitazone Protects Blood-Brain Barrier Integrity Following Diffuse Axonal Injury by Decreasing the Levels of Inflammatory Mediators Through a Caveolin-1-Dependent Pathway[J]. Inflammation, 2019, 42 (3): 841–856.
11. Liu RY, Wang JJ, Qiu X, et al. Acute hyperglycemia together with hematoma of high-glucose blood exacerbates neurological injury in a rat model of intracerebral hemorrhage[J]. Neurosci Bull, 2014, 30 (1): 90–98.
12. Liu WJ, Jiang HF, Rehman FU, et al. Lycium Barbarum Polysaccharides Decrease Hyperglycemia-Aggravated Ischemic Brain Injury through Maintaining Mitochondrial Fission and Fusion Balance[J]. Int J Biol Sci, 2017, 13 (7): 901–910.
13. Zhao JJ, Liu ZW, Wang B, et al. Inhibiting endogenous tissue plasminogen activator enhanced neuronal apoptosis and axonal injury after traumatic brain injury[J]. Neural Regen Res, 2020, 15 (4): 667–675.
14. Zhao YL, Song JN, Ma XD, et al. Rosiglitazone ameliorates diffuse axonal injury by reducing loss of tau and up-regulating caveolin-1 expression[J]. Neural Regen Res, 2016, 11 (6): 944–950.
15. Soslow RA, Dannenberg AJ, Rush D, et al. COX-2 is expressed in human pulmonary, colonic, and mammary tumors[J]. Cancer, 2000, 89 (12): 2637–2645.
16. Dong HJ, Shang CZ, Peng DW, et al. Curcumin attenuates ischemia-like injury induced IL-1β elevation in brain microvascular endothelial cells via inhibiting MAPK pathways and nuclear factor-κB activation[J]. Neurol Sci, 2014, 35 (9): 1387–1392.
17. Chen C, Huang Y, Xia P, et al. Long noncoding RNA Meg3 mediates ferroptosis induced by oxygen and glucose deprivation combined with hyperglycemia in rat brain microvascular endothelial cells, through modulating the p53/GPX4 axis[J]. Eur J Histochem, 2021, 65 (3).
18. Jin X, Sun Y, Xu J, et al. Caveolin-1 mediates tissue plasminogen activator-induced MMP-9 up-regulation in cultured brain microvascular endothelial cells[J]. J Neurochem, 2015, 132 (6): 724–730.
19. Miao Z, Dong Y, Fang W, et al. VEGF increases paracellular permeability in brain endothelial cells via upregulation of EphA2[J]. Anat Rec (Hoboken), 2014, 297 (5): 964–972.
20. Lin MN, Shang DS, Sun W, et al. Involvement of PI3K and ROCK signaling pathways in migration of bone marrow-derived mesenchymal stem cells through human brain microvascular endothelial cell monolayers[J]. Brain Res, 2013, 1513: 1–8.
21. Pang H, Huang T, Song J, et al. Inhibiting HMGB1 with Glycyrrhizic Acid Protects Brain Injury after DAI via Its Anti-Inflammatory Effect[J]. Mediators Inflamm, 2016, 2016: 4569521.

22. Xia X, Zhou C, Sun X, et al. Estrogen improved the regeneration of axons after subcortical axon injury via regulation of PI3K/Akt/CDK5/Tau pathway[J]. Brain Behav, 2020, 10 (9): e01777.
23. Svedung Wettervik T, Howells T, Ronne-Engström E, et al. High Arterial Glucose is Associated with Poor Pressure Autoregulation, High Cerebral Lactate/Pyruvate Ratio and Poor Outcome Following Traumatic Brain Injury[J]. Neurocrit Care, 2019, 31 (3): 526–533.
24. Zhang W, Hong J, Zheng W, et al. High glucose exacerbates neuroinflammation and apoptosis at the intermediate stage after post-traumatic brain injury[J]. Aging (Albany NY), 2021, 13 (12): 16088–16104.
25. Frank D, Melamed I, Gruenbaum BF, et al. Induction of Diffuse Axonal Brain Injury in Rats Based on Rotational Acceleration[J]. J Vis Exp, 2020, (159).
26. Obermeier B, Daneman R, Ransohoff RM. Development, maintenance and disruption of the blood-brain barrier[J]. Nat Med, 2013, 19 (12): 1584–1596.
27. Sweeney MD, Zhao Z, Montagne A, et al. Blood-Brain Barrier: From Physiology to Disease and Back[J]. Physiol Rev, 2019, 99 (1): 21–78.
28. Szot K, Góralczyk K, Michalska M, et al. The effects of humic water on endothelial cells under hyperglycemic conditions: inflammation-associated parameters[J]. Environ Geochem Health, 2019, 41 (3): 1577–1582.
29. Zhao Q, Zhang F, Yu Z, et al. HDAC3 inhibition prevents blood-brain barrier permeability through Nrf2 activation in type 2 diabetes male mice[J]. J Neuroinflammation, 2019, 16 (1): 103.
30. Meza CA, La Favor JD, Kim DH, et al. Endothelial Dysfunction: Is There a Hyperglycemia-Induced Imbalance of NOX and NOS?[J]. Int J Mol Sci, 2019, 20 (15).
31. Niu C, Chen Z, Kim KT, et al. Metformin alleviates hyperglycemia-induced endothelial impairment by downregulating autophagy via the Hedgehog pathway[J]. Autophagy, 2019, 15 (5): 843–870.
32. Strosznajder AK, Wójtowicz S, Jeżyna MJ, et al. Recent Insights on the Role of PPAR-β/δ in Neuroinflammation and Neurodegeneration, and Its Potential Target for Therapy[J]. Neuromolecular Med, 2021, 23 (1): 86–98.
33. Zhao F, Deng J, Xu X, et al. Aquaporin-4 deletion ameliorates hypoglycemia-induced BBB permeability by inhibiting inflammatory responses[J]. J Neuroinflammation, 2018, 15 (1): 157.
34. Tencer L, Burgermeister E, Ebert MP, et al. Rosiglitazone induces caveolin-1 by PPARgamma-dependent and PPRE-independent mechanisms: the role of EGF receptor signaling and its effect on cancer cell drug resistance[J]. Anticancer Res, 2008, 28 (2a): 895–906.
35. Llaverias G, Vázquez-Carrera M, Sánchez RM, et al. Rosiglitazone upregulates caveolin-1 expression in THP-1 cells through a PPAR-dependent mechanism[J]. J Lipid Res, 2004, 45 (11): 2015–2024.
36. Wu J, Zhou SL, Pi LH, et al. High glucose induces formation of tau hyperphosphorylation via Cav-1-mTOR pathway: A potential molecular mechanism for diabetes-induced cognitive dysfunction[J]. Oncotarget, 2017, 8 (25): 40843–40856.

37. Hayashi T, Juliet PA, Miyazaki A, et al. High glucose downregulates the number of caveolae in monocytes through oxidative stress from NADPH oxidase: implications for atherosclerosis[J]. Biochim Biophys Acta, 2007, 1772 (3): 364–372.
38. Tian C, Zhang R, Ye X, et al. Resveratrol ameliorates high-glucose-induced hyperpermeability mediated by caveolae via VEGF/KDR pathway[J]. Genes Nutr, 2013, 8 (2): 231–239.
39. Janket SJ, Jones JA, Meurman JH, et al. Oral infection, hyperglycemia, and endothelial dysfunction[J]. Oral Surg Oral Med Oral Pathol Oral Radiol Endod, 2008, 105 (2): 173–179.
40. Megawati ER, Meutia N, Lubis LD. The effect of hyperglycemia on the macrophages in the cell culture[J]. Folia Morphol (Warsz), 2021.
41. Samarghandian S, Borji A, Farkhondeh T. Attenuation of Oxidative Stress and Inflammation by Portulaca oleracea in Streptozotocin-Induced Diabetic Rats[J]. J Evid Based Complementary Altern Med, 2017, 22 (4): 562–566.
42. Campbell SJ, Deacon RM, Jiang Y, et al. Overexpression of IL-1beta by adenoviral-mediated gene transfer in the rat brain causes a prolonged hepatic chemokine response, axonal injury and the suppression of spontaneous behaviour[J]. Neurobiol Dis, 2007, 27 (2): 151–163.
43. Wang XX, Wu Z, Huang HF, et al. Caveolin-1, through its ability to negatively regulate TLR4, is a crucial determinant of MAPK activation in LPS-challenged mammary epithelial cells[J]. Asian Pac J Cancer Prev, 2013, 14 (4): 2295–2299.
44. Lee CY, Lai TY, Tsai MK, et al. The ubiquitin ligase ZNRF1 promotes caveolin-1 ubiquitination and degradation to modulate inflammation[J]. Nat Commun, 2017, 8: 15502.
45. Zhu T, Meng Q, Ji J, et al. TLR4 and Caveolin-1 in Monocytes Are Associated With Inflammatory Conditions in Diabetic Neuropathy[J]. Clin Transl Sci, 2017, 10 (3): 178–184.
46. Wang XM, Kim HP, Nakahira K, et al. The heme oxygenase-1/carbon monoxide pathway suppresses TLR4 signaling by regulating the interaction of TLR4 with caveolin-1[J]. J Immunol, 2009, 182 (6): 3809–3818.

Figures

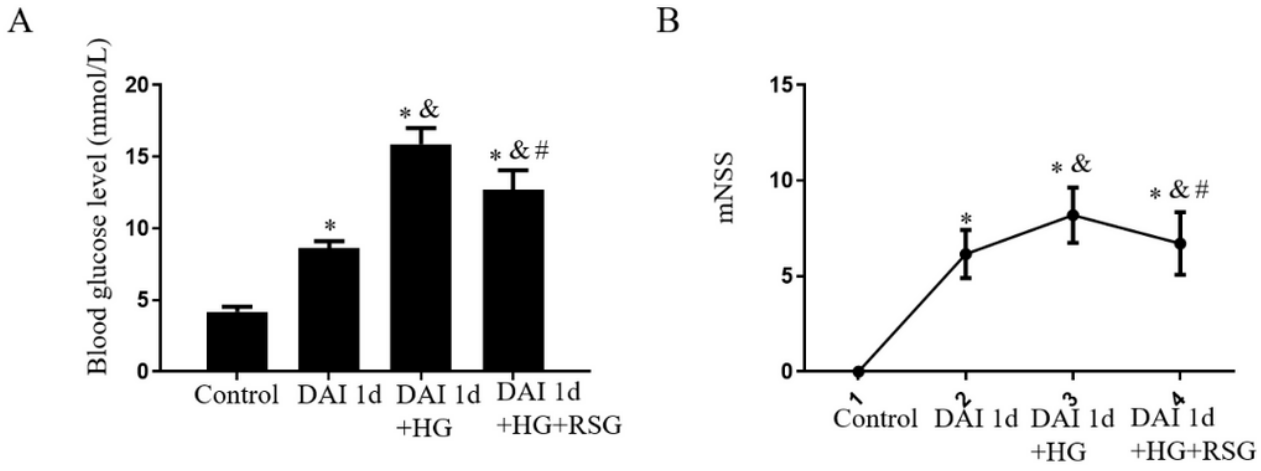

Figure 1

Glucose levels and neurological outcomes in rats subjected to hyperglycemia and RSG treatment after DAI. (A) Blood glucose levels (mM) in rats in each group. (B) The graph shows the mNSS score in each group. n = 6; $^{*}p$< 0.05, compared with the control group; $^{\&}p$< 0.05, compared with the DAI 1 d group; $^{\#}p$< 0.05, compared with the DAI 1 d+HG group.

Figure 2

The effects of hyperglycemia and PPARγ agonists on axonal injury were assessed by H&E staining, and the expression levels of NF-L, NF-H, and β-APP were determined through immunohistochemical staining (scale bar=100 μm) after DAI. n = 6; $^{*}p$< 0.05, compared with the control group; $^{\&}p$< 0.05, compared with the DAI 1 d group; $^{\#}p$< 0.05, compared with the DAI 1 d+HG group.

Figure 3

Effects of hyperglycemia and PPARγ agonists on cell apoptosis (× 40 magnification, n = 6) after DAI. n = 6; $^{*}p$< 0.05, compared with the control group; $^{\&}p$< 0.05, compared with the DAI 1 d group; $^{\#}p$< 0.05, compared with the DAI 1 d+HG group.

Figure 4

Effects of hyperglycemia and PPARγ agonists on the glial response (scale bar=100 μm) after DAI. n = 6; $^{*}p$< 0.05, compared with the control group; $^{\&}p$< 0.05, compared with the DAI 1 d group; $^{\#}p$< 0.05, compared with the DAI 1 d+HG group.

Figure 5

Dynamic PPARγ expression after DAI and OGD and the effects of hyperglycemia on PPARγ levels. (A) Dynamic PPARγ expression after DAI at different time points. n = 6; $^{*}p$< 0.05, compared with the control group; $^{\&}p$< 0.05, compared with the DAI 1 d group. (B) The effects of hyperglycemia on PPARγ expression in the rat cortex following DAI. n = 6; $^{*}p$< 0.05, compared with the control group. (C) Dynamic PPARγ expression after OGD at different time points. n = 6; $^{*}p$< 0.05, compared with the control group; $^{\&}p$< 0.05, $^{\#}p$>0.05, compared with the OGD 6 h group. (D) The effects of hyperglycemia on PPARγ expression in the

in vitro BBB model subjected to OGD and hyperglycemia. n = 6; $^{*}p$< 0.05, compared with the control group.

Figure 6

Effects of hyperglycemia and PPARγ agonists on the expression levels of TJ protein and BBB permeability after DAI in vivo. (A) ZO-1 expression levels assessed by immunofluorescence staining (× 40 magnification). (B) BBB permeability was assessed by Evans blue diffusion and BWC. n = 6; $^{*}p$< 0.05, compared with the control group; $^{\&}p$< 0.05, compared with the DAI 1 d group; $^{\#}p$< 0.05, compared with the DAI 1 d+HG group.

Figure 7

Effects of hyperglycemia and PPARγ agonists on the levels of TJ protein expression and BBB permeability after OGD in vitro. (A) The expression of occludin-1, ZO-1, and claudin-5 was determined by Western blotting. (B, C) TEER and HRP flux were measured to assess BBB integrity in vitro. n = 6; $^{*}p$< 0.05, compared with the control group; $^{\&}p$< 0.05, compared with the OGD 6 h group; $^{\#}p$< 0.05, compared with the OGD 6 h+HG group.

Figure 8

Effects of hyperglycemia and PPARγ agonists on the expression of caveolin-1, TNF-α, IL-1β, and IL-6 after DAI. (A) Caveolin-1 expression levels assessed by immunofluorescence staining (× 40 magnification). (B) The effects of hyperglycemia and PPARγ agonists on the levels of TNF-α, IL-1β, and IL-6 in the rat cortex following DAI were determined by ELISA. n = 6; $^{*}p$< 0.05, compared with the control group; $^{\&}p$< 0.05, compared with the DAI 1 d group; $^{\#}p$< 0.05, compared with the DAI 1 d+HG group.

Figure 9

In vitro, hyperglycemia disrupted the BBB model by increasing the levels of inflammatory factors through the PPARγ/caveolin-1/TLR4 pathway. (A) The expression levels of caveolin-1 and TLR4 were determined by Western blot. n = 6; $^{*}p$< 0.05, compared with the control group; $^{\&}p$< 0.05, compared with the OGD 6 h group; $^{\#}p$0.05, compared with the OGD 6 h+HG group. (B) The expression levels of TLR4 and Myd88 were determined by Western blot. n = 6; $^{*}p$< 0.05, compared with OGD 6 h+HG+RSG. (C) The levels of

TNF-α, IL-1β, and IL-6 after OGD, hyperglycemia induction, and RSG treatment were determined by ELISA. n = 6; $^{*}p$< 0.05, compared with the control group; $^{\&}p$< 0.05, compared with the OGD 6 h group; $^{\#}p$ 0.05, compared with the OGD 6 h+HG group. (D) The levels of TNF-α, IL-1β, and IL-6 after OGD, hyperglycemia induction, Cav-1 siRNA, and RSG treatment were determined by ELISA. n = 6; $^{*}p$< 0.05, compared with OGD 6 h+HG+RSG.